Resonances in $\bar{p}p \to \omega\eta$ from 600 to 1940 MeV/c

A.V. Anisovich [c], C.A. Baker [a], C.J. Batty [a], D.V. Bugg [b], V.A. Nikonov [c], A.V. Sarantsev [c], V.V. Sarantsev [c], B.S. Zou [b,1]

[a] *Rutherford Appleton Laboratory, Chilton, Didcot OX11 0QX, UK*

[b] *Queen Mary and Westfield College, London E1 4NS, UK*

[c] *PNPI, Gatchina, St. Petersburg district, Russia 188350*

Abstract

Data on $\bar{p}p \to \omega\eta$ from the Crystal Barrel experiment are presented in the mass range 1960 to 2410 MeV. A partial wave analysis confirms a number of resonances previously reported in an analysis of $\omega\pi^0\pi^0$ data. In particular the $\omega\eta$ data define the parameters of a 1^{+-} $I = 0$ resonance at 2000 ± 20 MeV better than the earlier data. A combined analysis with the $\omega\pi^0\pi^0$ data is reported.

[1] IHEP, Beijing 100039, China

The channel $\bar{p}p \to \omega\eta$ is investigated, in a search for s-channel resonances with isospin $I = 0$ and charge conjugation $C = -1$. Data are obtained by the Crystal Barrel collaboration in a study of the 5γ final state, where $\omega \to \pi^0\gamma$. These data complement earlier data on the $\omega\pi^0\pi^0$ channel, which has the same isospin and C parity.

The experiment was carried out at LEAR, using $\bar{p}$ beams from 600 to 1940 MeV/c, corresponding to the mass range 1960–2410 MeV. The detector has been described fully before [1], so the experimental set-up is described only briefly. The $\bar{p}$ beam interacts in a liquid hydrogen target 4.4 cm long, situated at the centre of the detector. Two veto counters downstream of the target provide an on-line trigger for an interacting $\bar{p}$. Charged particle detectors (silicon vertex detector, multiwire chambers and jet drift chambers) cover 98% of the solid angle and serve as on-line and off-line vetos, providing a trigger for neutral final states. The beam intensity was typically 2×10^5/s and the trigger rate for neutral final states typically 60/s. A barrel of 1380 CsI crystals detects photon over 98% of 4π solid angle with an angular resolution of 20 mrad in both polar angle and azimuth. The γ detection is efficient down to energies of 20 MeV. This is important in the present measurement, since some photons from $\omega \to \pi^0\gamma$ have very low lab energies. The energy resolution is given by $\Delta E/E = 2.5\%/E^{1/4}$, with E in GeV. On-line, the energy from all CsI crystals is summed and provides a trigger for events with a total energy within 200 MeV of that expected for $\bar{p}p$ interactions [2].

In the off-line analysis, events are selected containing exactly 5 photon showers and are subjected to kinematic fitting. In the selection procedure, events are first fitted kinematically to 5γ, then $\eta\pi^0\gamma$ and finally $\omega\eta$. Almost the entire background arises from $\eta\pi^0\pi^0$ events after the loss of one photon. The effect of this background and others has been studied using a Monte Carlo simulation with GEANT; a variety of alternative strategies for data selection have been tested. After tuning to minimise all backgrounds, the following cuts are selected: (i) Confidence Level (CL) for $\omega\eta > 10\%$, (ii) $CL(\pi^0\pi^0\gamma) < 0.1\%$ to reject $\omega\pi^0$, (iii) $CL(\omega\eta) > 0.5$ times the confidence level of any other fitted channel, e.g. $\omega\eta'$; such channels have much lower branching fractions than $\omega\eta$; (iv) $CL(\omega\eta) > 0.8 \times CL(5\gamma)$; this is a minor refinement to check that the initial selection of 5γ events is secure. Numbers of events, reconstruction efficiencies and estimated backgrounds are shown in Table 1.

Fig. 1(a) shows the $\pi^0\gamma$ mass distribution at one beam momentum, 1800 MeV/c, for events fitted to $\eta\pi^0\gamma$. There is a clear $\omega(782)$ signal with a mass within 1.5 MeV of the PDG value [3]. Fig. 1(b) shows the $\gamma\gamma$ mass distribution around the mass region of the η for events fitted to $\omega\gamma\gamma$. Again there is a clear η signal within 2 MeV of the standard value. These results check that the reconstruction energy is assessed correctly. The mass resolution has a standard deviation of 17 MeV for the ω and 15 MeV for the η.

Momentum (MeV/c)	CM Energy MeV	Events	ϵ %	BG %
600	1962	3767	26.8	4
900	2050	13653	26.8	6
1050	2098	9216	26.6	7
1200	2149	11748	26.3	8
1350	2201	7127	25.7	9
1525	2263	4420	24.8	10
1642	2304	4742	24.2	11
1800	2360	4332	23.4	13
1940	2409	4614	22.6	14

Table 1
Numbers of $\omega\eta$ events after background subtraction, reconstruction efficiency ϵ and estimated backgrounds (BG). Column 2 shows the total energy available in the centre of mass system.

Production angular distributions are shown in Fig. 2 at all momenta, together with the results of the partial wave fit. Results are uncorrected for acceptance, which is included in the maximum likelihood fit. The data are displayed over the whole range $\cos\theta = -1$ to $+1$. Charge conjugation invariance demands that the angular distribution should be symmetric forward-backward in the centre of mass frame. After allowance for the acceptance, the data are consistent with this requirement within errors. This again checks that particles are correctly reconstructed without significant biases between high energy (forwards in the lab system) and low energy. Angular distributions require waves up to orbital angular momentum $\ell = 3$. Integrated cross sections are shown in Fig. 3 and compared with the partial wave fit.

The partial wave analysis fits the full process of production and decay of the ω using relativistic tensor expressions; J^P up to 5^- are tried. Background is taken from the Monte Carlo simulation of the competing channels and is adjusted at each beam momentum to the level of estimated backgrounds. The cross section is summed over photon polarisations from $\omega \to \pi^0\gamma$ decay. The decay angular distribution of the ω gives limited information about its spin alignment between helicities 0 and ± 1. However, a significant proportion of this spin information is carried away in the unmeasured polarisation of the photon.

An earlier analysis of the $\omega\pi^0\pi^0$ channel, having the same quantum numbers $I = 0$ and $C = -1$, has located many of the $q\bar{q}$ resonances expected in this mass range [4]. Because of the limited statistics of the $\omega\eta$ channel, the partial wave analysis takes as a starting point the resonances previously observed in $\omega\pi^0\pi^0$, where the statistics are larger by a factor 3 to 8, depending on momentum. The analysis is made at all beam momenta simultaneously in terms of a sum of s-channel resonances. This introduces the important constraint of analyticity, since Breit-Wigner resonance amplitudes are analytic functions of s.

The $\omega\eta$ data fit immediately to the resonances reported earlier, with very little adjustment of masses and widths. There is one case where the present data lead to a significant improvement in resonance parameters. This is for the lower of two 1^{+-} resonances. For $\omega\pi^0\pi^0$ data it was fitted to a mass of 2020 ± 25 MeV with $\Gamma = 180^{+45}_{-25}$ MeV. For the present $\omega\eta$ data, where this particular resonance appears more strongly, fitted values are 1995 ± 20 MeV with $\Gamma = 205 \pm 20$ MeV.

We have carried out an analysis of the $\omega\eta$ data alone, allowing masses and widths of resonances to adjust freely. We have also carried out a combined analysis with the $\omega\pi^0\pi^0$ data. Results of both fits are displayed in Table 2. Fig. 4 shows the intensities of partial waves fitted to the $\omega\eta$ data in the combined fit.

We now comment on individual resonances. The upper 1^{+-} resonance at 2270 MeV is needed in the $\omega\eta$ data, Fig. 4(h), in decays to $\omega\eta$ $^3S_1$. It is closely consistent in mass with that fitted to $\omega\pi^0\pi^0$; however, it is stronger in $\omega\pi^0\pi^0$. It also couples strongly to $^3D_1$ decays with $D/S = 2.8 \pm 0.5$ after factoring out the effect of the centrifugal barrier. It is responsible for the dip at 2.25 GeV in Fig. 4(i). The lower 1^{+-} resonance decays dominantly to $\omega\eta$ with $L = 2$, i.e. to $^3D_1$; it is clearly visible in Fig. 4(i). Its ratio of coupling constants in D and S-wave decays is $D/S = -4.8 \pm 0.8$. For all other resonances, only decays to the lower of the allowed L values are significant.

For $J^P = 3^{+-}$, the $\omega\eta$ data provide only marginal evidence for the resonance observed in $\omega\pi^0\pi^0$ at 2275 MeV; if this resonance is included in the fit to $\omega\eta$, log likelihood improves by 17. A further 3^{+-} resonance is expected around 2030 MeV. Again, if it is included in the fit to $\omega\eta$, log likelihood improves by 17, which is not definitive in the absence of evidence from $\omega\pi^0\pi^0$ data.

For $J^{PC} = 1^{--}$, there is a definite requirement in the present data for poles around 1930 and 2145 MeV. The former is at the bottom of the available mass range and its mass and width are not well defined; with a mass of 1930 MeV, it cannot be distinguished from the possible effect of the $\bar{p}p$ threshold. The parameters of the state at 2150 MeV optimise close to those found for $\omega\pi^0\pi^0$, but its significance in the $\omega\pi^0\pi^0$ data is larger because of the higher statistics. In fitting the latter data, there was evidence for a third resonance at 2305

J^{PC}	Mass M (MeV)	Width Γ (MeV)	ΔS	Mass (MeV)	Width (MeV)
1^{+-}	1995 ± 20	205 ± 20	209	2000 ± 20	205 ± 20
1^{+-}	2270 ± 15	150 ± 45	76	2270 ± 15	175 ± 30
3^{+-}	2255 ± 45	155 ± 45	17	2270 ± 30	170 ± 30
1^{--}	(1930)	(150)	281	(1930)	(155)
1^{--}	2150 ± 20	235 ± 30	90	2145 ± 15	215 ± 25
1^{--}	2295 ± 60	395 ± 90	53	2300 ± 45	360 ± 55
2^{--}	1960 ± 35	170 ± 55	34	1960 ± 35	170 ± 55
2^{--}	2245 ± 70	210 ± 75	94	2205 ± 45	220 ± 45
3^{--}	1955 ± 30	165 ± 30	230	1955 ± 30	165 ± 30
3^{--}	2175 ± 40	230 ± 55	46	2180 ± 30	290 ± 35
3^{--}	2250 ± 20	200 ± 40	187	2255 ± 25	185 ± 30

Table 2
Resonances fitted to the data. Columns 2 and 3 show parameters fitted to $\omega\eta$ data alone. Values in paranethese are fixed. The next column shows changes in S =log likelihood when each resonance is omitted from this fit and others are re-optimised. Our definition of log likelihood is such that it changes by 0.5 for a one standard devation change in one parameter. The last two columns show resonance parameters from the combined fit to $\omega\eta$ and $\omega\pi^0\pi^0$ data.

MeV. This state appears to be needed also by $\omega\eta$ data, giving an improvment in log likelihood of 53. A scan of its mass and width gives values consistent with $\omega\pi^0\pi^0$ data, but with large errors. However, this state is sufficiently weak that it does not appear clearly in Fig. 4(a) and (b).

For $J^{PC} = 2^{--}$, the $\omega\eta$ data require a weak resonance at 1960 ± 35 MeV; it was also observed in the fit to $\omega\pi^0\pi^0$, but with less well defined mass. The latter data also demanded strongly the presence of a second 2^{--} resonance at higher masses around 2180 MeV. If this is included in the fit to $\omega\eta$, there is a large improvement of 94 in log likelihood; the mass optimises somewhat higher than for $\omega\pi^0\pi^0$, at 2245 MeV, but with a quite large error of ± 70 MeV.

For$J^{PC} = 3^{--}$, three well defined resonances are required in fitting either $\omega\eta$ or $\omega\pi^0\pi^0$, and their masses and widths agree well between the two data sets. The lowest $^3D_3$ state appears strongly in Fig. 4(d). The highest 3^{--} state contributes strongly to $^3G_3$ in Fig. 4(e). Evidence for the intermediate $^3D_3$ state in $\omega\eta$ is tentative; omitting it, log likelihood changes by 46. However, it does not appear distinctively in either Fig. 4(d) or (e).

Further 4^{--} and 5^{--} resonances are to be expected around 2300 MeV, and there was tentative evidence for the presence of the 4^{--} state in fitting $\omega\pi^0\pi^0$. For $\omega\eta$, both 4^{--} and 5^{--} give small but significant contributions, but they are too small to determine resonance masses and widths reliably. These are set at $M = 2300$ MeV and $\Gamma = 350$ MeV. Omitting $^3G_4$ and $^3G_5$ amplitudes has little effect on other partial waves.

In summary, the $\omega\eta$ data agree closely with $\omega\pi^0\pi^0$ in the determination of resonance parameters. Although statistics are substantially lower than for $\omega\pi^0\pi^0$, they provide useful confirmation of resonance parameters; in particular, they improve the determination of the mass and width of the 1^{+-} state at 2000 ± 20 MeV. The combined analysis with $\omega\pi^0\pi^0$ data locates many of the expected $q\bar{q}$ states up to spin 3. However, the expected 3^{+-} state around 2030 MeV is not obviously present in either set of data. The evidence for 4^{--} and 5^{--} states is not yet definitive.

1 Acknowledgement

We thank the Crystal Barrel Collaboration for allowing use of the data. We acknowledge financial support from the British Particle Physics and Astronomy Research Council (PPARC). We wish to thank Prof. V. V. Anisovich for helpful discussions. The St. Petersburg group wishes to acknowledge financial support from PPARC and INTAS grant RFBR 95-0267.

References

[1] E. Aker et al., Nucl. Instr. A321 (1992) 69.

[2] C.A. Baker, N.P . Hessey, C.N. Pinder and C.J. Batty, Nucl. Instr. A394 (1997) 180.

[3] Particle Data Group (PDG), Euro. Phys. Journ. C15 (2000) 1.

[4] A.V. Anisovich et al., Phys. Lett. B476 (1999) 15.

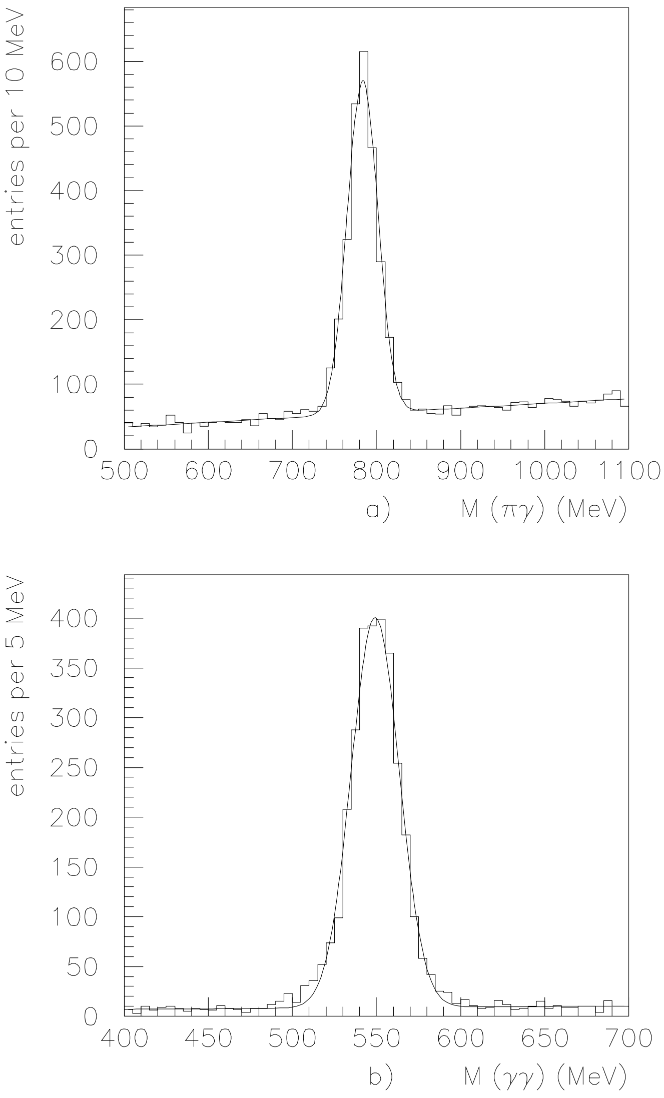

Fig. 1. (a) Mass distribution of $\pi^0\gamma$ pairs after a kinematic fit to $\eta\pi^0\gamma$; (b) mass distribution of $\gamma\gamma$ pairs around the $\eta(550)$ after a kinematic fit to $\omega\gamma\gamma$.

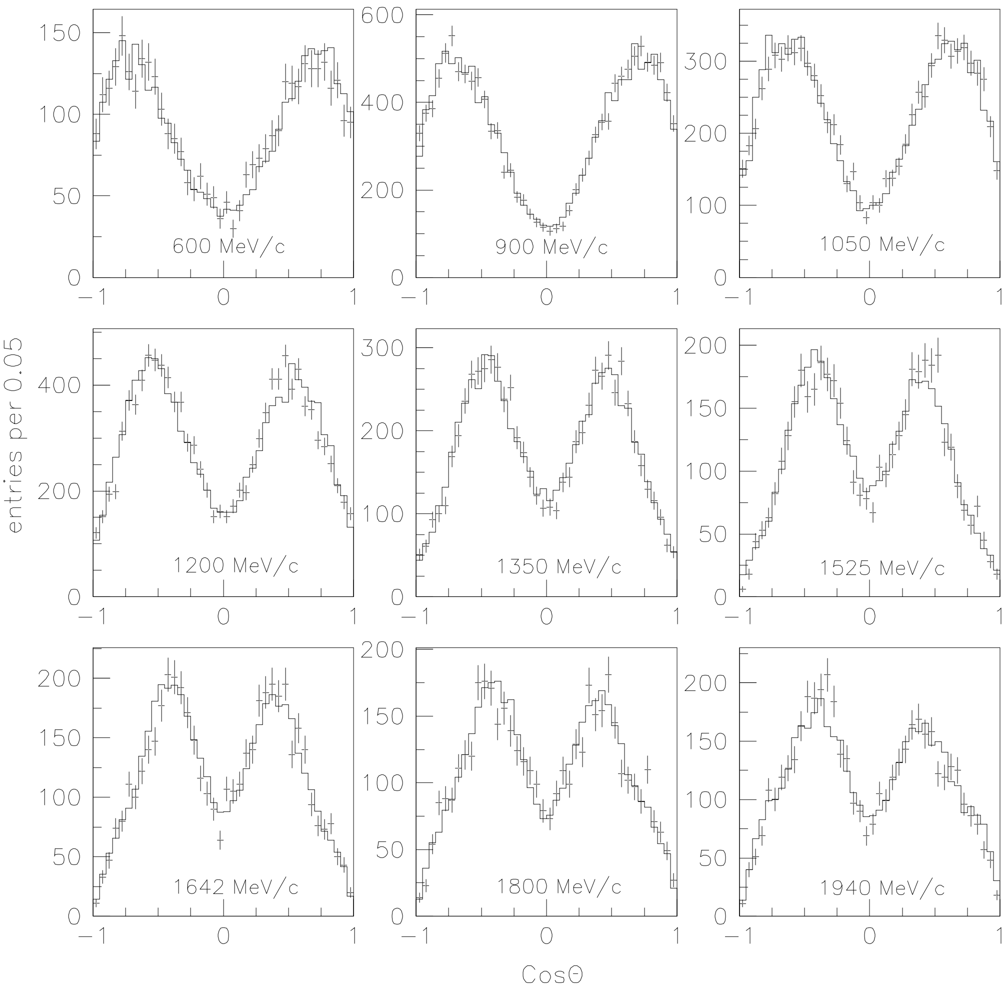

Fig. 2. Production angular distributions in the centre of mass frame for $\omega\eta$, uncorrected for acceptance. Histograms show the partial wave fit.

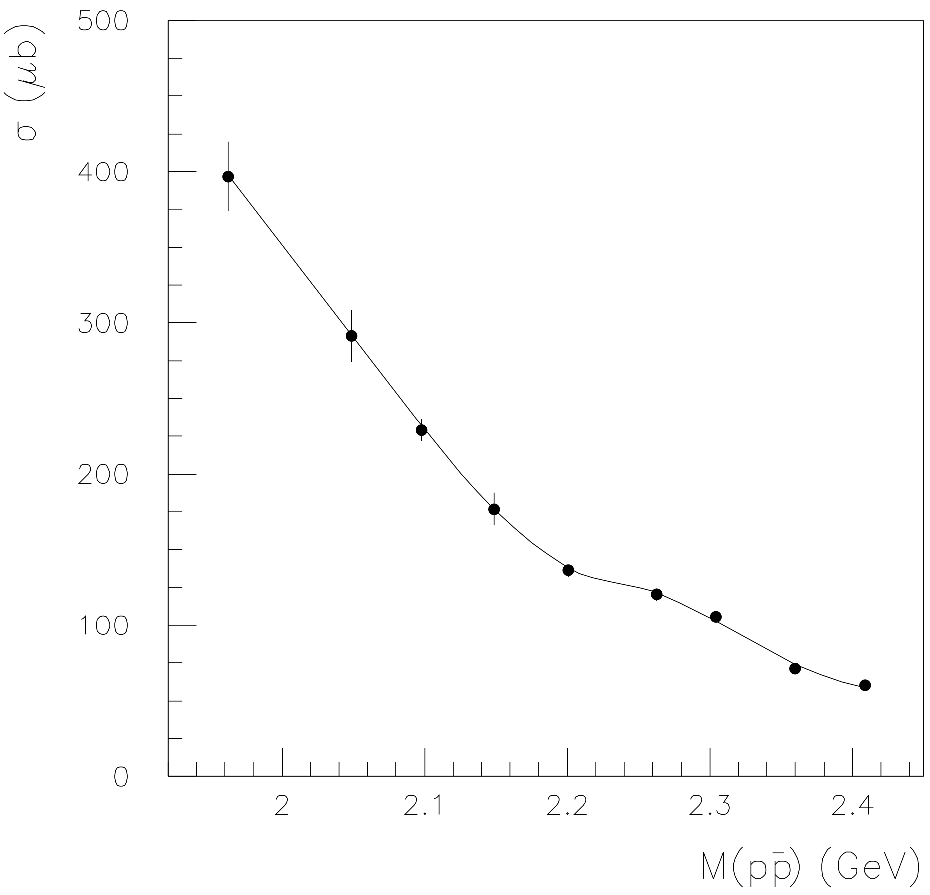

Fig. 3. Integrated cross sections for $\omega\eta$, corrected for branching ratios of $\omega \to \pi^0\gamma$ and $\eta \to \gamma\gamma$ and for acceptance. Histograms show the partial wave fit.

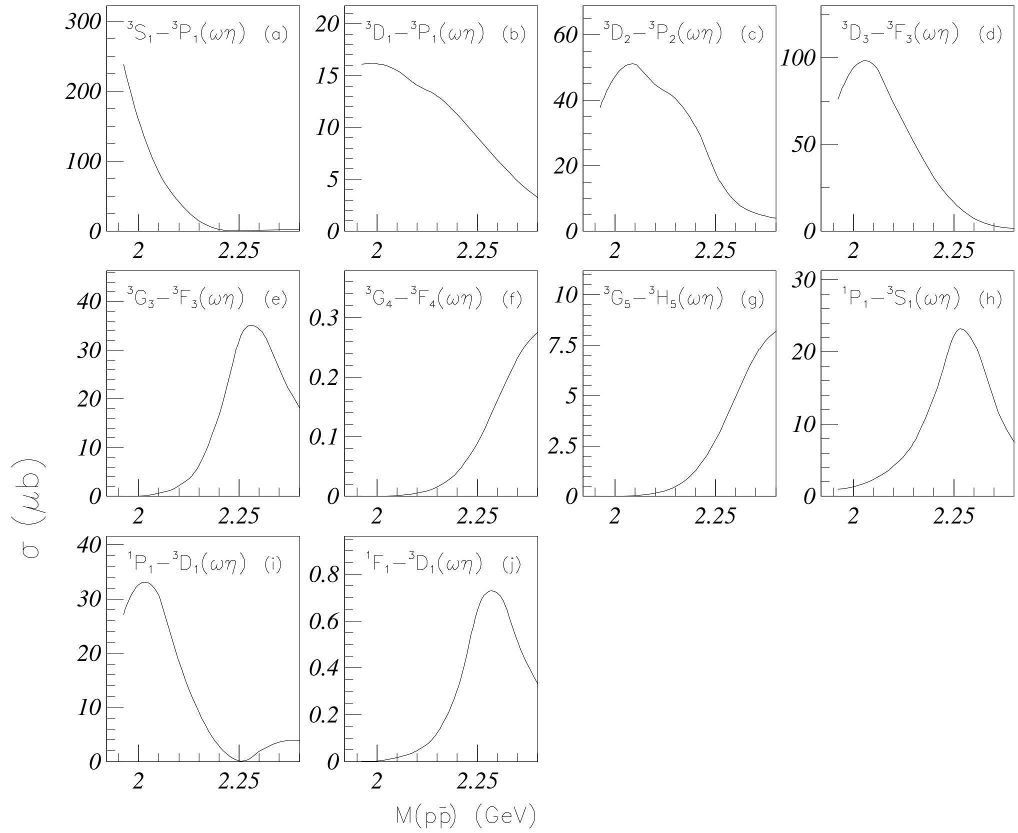

Fig. 4. Intensities of partial waves fitted to $\omega\eta$ in a combined fit to $\omega\eta$ and $\omega\pi^0\pi^0$.